INCREASE IN LONGIVITY OF IMPLANTABLE NEURAL DEVICE USING NOVEL MATERIAL

Sandeep Negi[1,2], Christopher K. Nguyen[3], David J. Warren[2], Stuart F. Cogan[3], Florian Solzbacher[2], and Rajmohan Bhandari[1,2]*
[1]Blackrock Neurotech, Salt Lake City, Utah, USA
[2]University of Utah, Salt Lake City, Utah, USA
[3]University of Texas at Dallas, Richardson, Texas, USA

ABSTRACT

Brain-Computer Interface (BCI) utilizes implantable devices with intricate three-dimensional geometries, such as the Utah electrode array (UEA), which are expected to endure for multiple decades. The UEA is coated with an encapsulation biomaterial, parylene-C. Parylene-C has been the gold standard for encapsulating neural and biomedical implants due to its excellent combination of biocompatibility, electrical properties, and chemical inertness. However, over time, the recording capabilities of long-term neural implants encapsulated with parylene-C overtime show signs of degradation. To overcome this challenge, we evaluated a new encapsulation material: amorphous silicon carbide (a-SiC). This material is designed to extend the long-term stability and extend the implantable lifetime, aligning with the lifetime expectations for conventional cochlear implant electrodes.

KEYWORDS

Brain-Computer Interface, Neural Device, Biomaterials, Longevity, Silicon Carbide.

INTRODUCTION

A neural prosthesis, also referred to as a neural implant or BCI, is a device that interfaces with the nervous system to restore lost sensory or motor functions. These prostheses are specifically designed to bypass damaged neural pathways and facilitate direct communication between the brain or nervous system and external devices or artificial limbs. Neural prosthesis offers tremendous potential for enhancing the quality of life for individuals with neurological disorders or disabilities. Ongoing research and advancements in neural engineering continue to broaden the capabilities and applications of these remarkable devices.

Neural electrodes have played a pivotal role in the exploration and understanding of the human brain. In the 1950s, tungsten microwires were extensively utilized for brain studies. Subsequent advancement in technology, drawing from integrated circuit technology and materials science, have significantly expanded the field of neurotechnology, providing new avenues for exploring the human brain. This progress led to the development of silicon-based electrodes, with notable examples including the Michigan electrodes in 1970s and Utah array in 1990s.

One of the primary design requirements for implantable neural devices is their longevity within the human brain, spanning several decades. The Utah electrode array (UEA) architecture represents a milestone in this field, being one of the devices cleared for human use and serving as a cornerstone in numerous studies involving BCI and peripheral neural implants. Despite decades of development, microelectrode arrays have yet to achieve the level of reliability and electrode interface stability necessary for chronic applications extending over the lifetimes of patients. Basic science studies, particularly those focused on neural recording, face challenges due to the rapid decline in the quantity and quality of neural signals over time. For example, the UEA typically lasts only around 8 years before performance degradation occurs. One significant reason for this degradation is the cerebrospinal fluid (CSF) eventually breaking through the encapsulation layer of the neural devices, causing short circuits in the electrodes [1]. The encapsulation layer of the UEA is composed of a biocompatible polymer, parylene-C [2]. Consequently, the development of suitable encapsulation materials for neural electrodes has been an ongoing effort for decades.

Silicon carbide (SiC) possesses inherent properties that make it an excellent material for encapsulating implantable devices. SiC exhibits exceptional resistance to water vapor transmission compared to many other commonly used materials across various applications. Known for its high chemical inertness, mechanical strength, and thermal stability, SiC is highly resistant to water vapor penetration. This property renders SiC suitable for applications where exposure to moisture is a concern, such as in semiconductor processing, aerospace components, and high-temperature applications. SiC is a novel material in the biomedical field, offering all the advantages of Parylene-C while showcasing vastly superior dielectric properties, thus creating a much longer-lasting and more electrically stable biomedical implant. This encapsulation layer scheme can seamlessly integrate into our existing fabrication process flow for the UEA, alleviating any concerns about manufacturability. SiC, as an encapsulation layer, is compatible with various surfaces (metal, semiconductor, polymer, and ceramic) and devices with integrated wireless components, making it ideal for coating complex medical devices intended for long-term implantation.

METHODS

The UEA consists of a 10x10 square grid of 1.5 mm long electrodes with 400 µm spacing between them as shown in Figure 1. The UEA features an out-of-plane structure with a high aspect ratio of 15:1. The fabrication process of 10x10 configured UEA, along with stability studies, has been reported elsewhere [3-5]. The implementation of SiC on UEAs is a collaboration between Blackrock Neurotech (BRN) and the University of Texas at Dallas (UTD). While BRN manufactures UEAs, and UTD advances SiC processing.

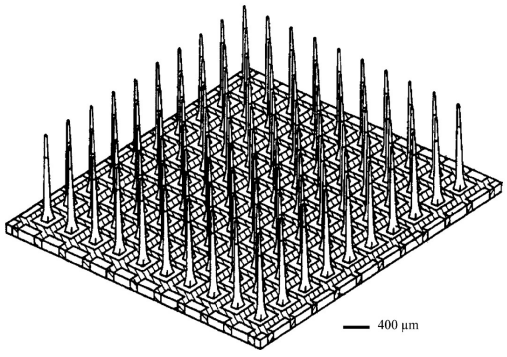

Figure 1: Schematic image of the Utah Electrode Array (UEA)

The SiC film is deposited on the UEAs via plasma-enhanced chemical vapor deposition (PECVD) on a Plasma-Therm Unaxis 790 Series PECVD system. Deposition occurs at 325°C, 1000 mTorr, and

978-1-940470-05-4/HH2024/$25©2024TRF
DOI 10.31438/TRF.HH2024.112

200 W, with a gas ratio of 1:3 SiH_4:CH_4, and 800 sccm Ar [6-9]. Monitor Si wafers were included to measure the relative thickness and film stress of each deposition. Thickness measurements of the SiC film along the shafts were conducted using focused ion beam (FIB) milling and physically fracturing the array. Scanning electron microscopy (SEM) images were obtained using a Zeiss Supra 40 microscope.

The UEAs are punctured through a 7-µm thick sheet of Al foil coated with a 3-µm layer of Parylene-C, which adheres around the shafts, serving as a hard mask to expose only the tips as electrode sites. The tips undergo de-insulation via reactive ion etching (RIE) using a Trion Sirus-T2 RIE system, employing capacitively coupled plasma (CCP) with a 50-in2 platen. We conducted a study on the combination of SF6 and O2 gas flow in the plasma to enhance the etch selectivity of SiC over Si, aiming to preserve the underlying architecture and minimize over-etching. While still covered with Al foil, the UEAs are then coated with a sputtered iridium oxide film (SIROF) using an AJA ATC 2200 DC magnetron sputtering system to deposit electro-active coatings at the electrode site. This coating consists of a 60-nm Ti adhesion layer followed by a 250-nm SIROF layer, assisted by H2O vapor, as depicted in Figure 2

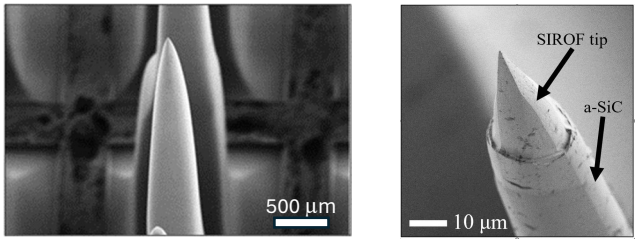

Figure 2: SEM micrograph of (a) a-SiC coated electrode of the UEA and (b) post etching of a-SiC from electrode tips exposing SIROF on the electrode tip and SiC on the shank.

The stability of SiC encapsulation stability on UEAs were assessed through electrochemical measurements. All electrochemistry was conducted using a Gamry Interface 1000E in a three-electrode configuration in air-equilibrated PBS. We employed Ag/AgCl as the reference electrode and a large-area Pt wire as the counter electrode. Electrochemical impedance spectroscopy (EIS) was utilized to measure electrode impedance across frequencies ranging from 10^{-1} to 10^5 Hz. Cyclic voltammetry (CV) was employed to measure the current response of the electrode when cycling the potential between -0.6 to 0.8 V—the water electrolysis window of SIROF. All CV measurements were performed at a scan rate of 50 mV/s, ensuring a slow enough sweep to fully access the SIROF film on the electrode tip. The purpose of CVs was to determine the charge storage capacity (CSC) in the electrodes during potential cycling.

The performance of a-SiC-encapsulated UEAs was evaluated in the motor cortex of a rat model for long-term neural stimulation. The study utilized 4×4-configured UEAs (shown in Figure 2) that were encapsulated with a-SiC. The geometric surface area of the electrodes was approximately 5,000 μm^2, and the electrodes were coated with SIROF. Some arrays were soaked in PBS at 37°C as a negative control to remove biotic factors. Weekly electrochemical evaluations and microstimulations were performed on UEAs encapsulated with a-SiC. Adjustments to the microstimulation protocol were made due to instrumentation limitations, aimed at preventing irreversible electrochemical reactions, and mitigating tissue damage. The study showcased the electrochemical stability of UEAs encapsulated with a-SiC post-implantation. The SiC-coated UEAs were implanted over a period of 20 weeks, during which animals underwent weekly electrochemical measurements and intracortical microstimulations to monitor the statuses and functionalities of the implanted UEAs.

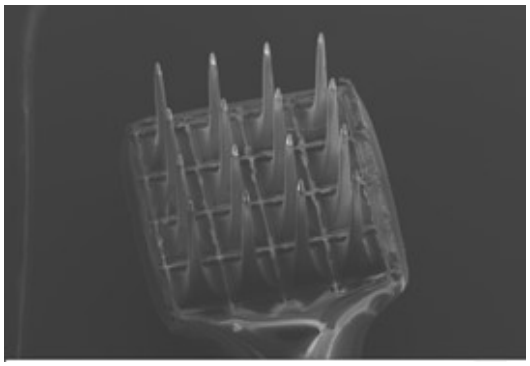

Figure 3: SEM micrograph of 4x4 UEA. The pitch between the shanks is 400um in both directions.

The a-SiC coated UEA was implanted in a cat, and five stimulation sessions were performed. In each session, we stimulated 54 out of the 96 electrodes. The stimulation was conducted sequentially, starting with the simultaneous stimulation of the first seven channels, followed by the subsequent groups of seven channels until reaching the final group of six channels. This arrangement totaled 54 stimulated channels (6 * 7 + 2 * 6 = 54). However, channels with impedance below 5 kΩ or above 500 kΩ were excluded from stimulation. Consequently, channels 3, 4, 5, 29, 30, 40, and 42 were not stimulated. Channels beyond 61 were also not stimulated. The stimulation protocol involved balanced, biphasic, cathodic-first constant current pulses of 100 µA with a pulse width of 200 µs per phase and a 100 µs interphase period. After stimulating each group with a single pulse, the next group was stimulated, and this process was repeated until all groups were stimulated. The same order of stimulation was repeated for each session. Before and after each stimulation session, impedance measurements were recorded for all 96 channels. This measurement was repeated five times both before and after stimulation. Specifically, impedance was tested using a 1 kHz sine wave current of 10 nA with 300 cycles of the sine wave.

RESULTS AND DISCUSSION

As expected, a-SiC deposition on planar structure yielded different thicknesses compared to 3D structures such as the UEA. Monitor wafers exhibited thicknesses of 548.55 ± 15.22 nm and film stress of -128.61 ±18.57 MPa. Measurement of a-SiC thickness on UEAs was conducted through cross-sectional milling via FIB. In Figure 4(a), SiC encapsulation of the UEA tip is depicted, while Figure 4(b) illustrates a clear distinction in interface and morphology between Si and a-SiC

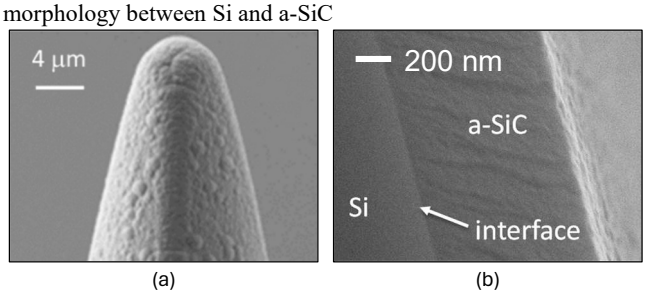

Figure 4. SEM images of SiC on UEA. (a) Conformal coating of a-SiC on the tip; (b) Interface between SiC and Si on the shaft. The cross-section of the interface was formed by FIB milling.

Table 1 presents average thickness measurements obtained from SEM images in Figure 3. As indicated in the table, there is a

significant decrease in the thickness of the a-SiC layer from the tip to the base of the shaft. The length of the shaft is approximately 1.5 mm.

Table 1: Average thickness (± SD) of SiC along the UEA.

Shaft Location	Average Thickness (± *SD*) (µm)
Tip	4.88 ± 0.68
Upper Half	1.49 ± 0.14
Lower Half	1.17 ± 0.20
Base	0.51 ± 0.14

Figure 5 shows the stability of the a-SiC coated UEA in accelerated settings (87 C).

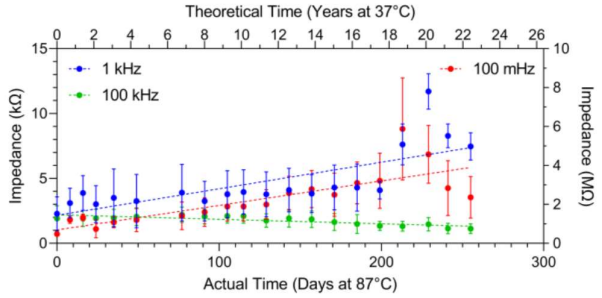

Figure 5: Average electrochemical impedance at different frequencies showing performance stability for more than 22 years.

Figure 6 shows the stability of the a-SiC coated UEA in accelerated settings (87 C).

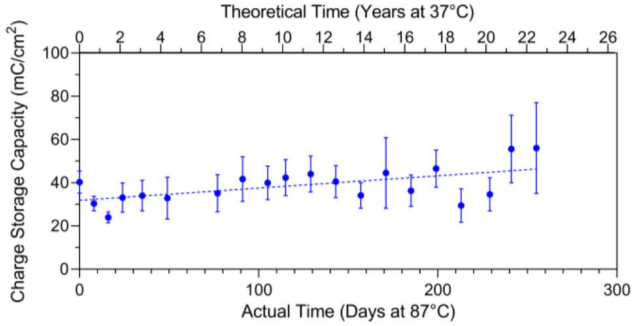

Figure 6: Average charge storage capacity calculated from CVs.

Figure 7 displays the stability of the a-SiC coated UEA under accelerated conditions (87°C). Stability is assessed through measurements of electrode impedance at 1 kHz and charge storage capacity. Based on these results, it can be inferred that the device will exhibit stability for more than 22 years at 37°C.

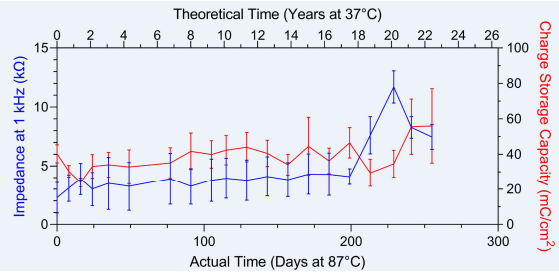

Figure 7: Combined impedance and CSC of the UEAs over time show stability over 22+ years.

Figure 8 presents the Bode plot of electrode impedance as a function of frequency. The graph illustrates the impedance of the implanted electrode over a period of 20 weeks and compares it to data collected in in vitro settings. Upon implantation, there is a notable increase in impedance, which may be attributed to the presence of different media and the formation of scar tissue around the electrode.

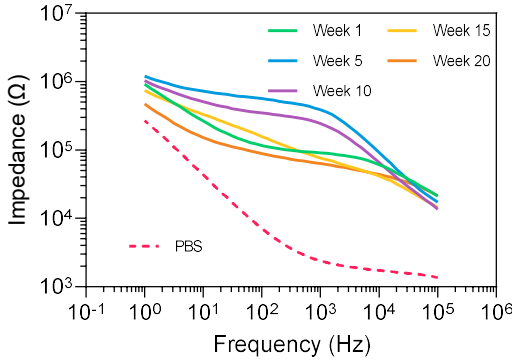

Figure 8: Representative bode plot of the electrodes implanted in rat's motor cortex for 20 weeks.

Figure 9 displays the cyclic voltammograms of the electrode in PBS and after 20 weeks of implantation. The CVs appear to show stable behavior over the measured period.

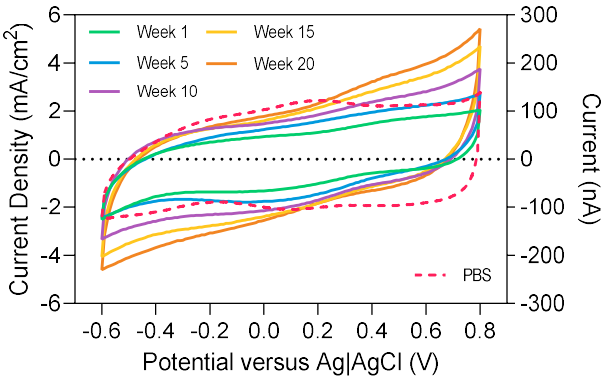

Figure 9: Representative cyclic voltammograms of an electrode implanted in rat's cortex showing data for 20 weeks.

Figure 10 illustrates the relative change in electrode impedance over time in the electrodes implanted in the cat. This data was compared with Chen's data, which involved electrodes with Parylene-C insulation [10]. The impedance values demonstrate a gradual increase with time. Around the 13th week, notable changes in impedance were observed for both unstimulated (control, green line and region) and stimulated electrodes (red line and region). Particularly, the stimulated electrodes exhibited an initial dip followed by a gradual increase in impedance. The data collected with SiC insulation suggests that SiC is maintaining its integrity better than Parylene-C insulation. One could hypothesize that the increase in impedance over time is attributed to the encapsulation of the electrode surface with fibrotic tissue from the foreign body response (FBR). Additionally, it's plausible to consider that for Parylene-C insulation, degradation of the insulation might be more prevalent than the increase due to the FBR, resulting in lower impedances over time. In contrast, the impedance data for a-SiC

insulation does not exhibit a decrease, leading to the hypothesis that the SiC insulation is not degrading. Instead, the increase in impedance may be attributed to the FBR becoming more apparent with SiC insulation.

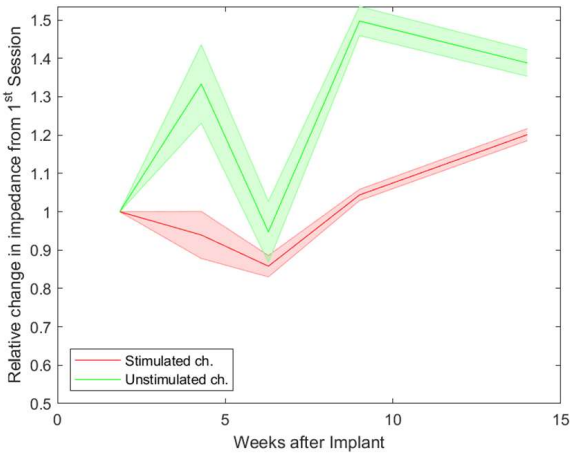

Figure 10: The relative change in electrode impedance over time for stimulated and unstimulated electrodes.

The most informative result is the change in impedance across sessions, relative to the impedance of the first session. In our analysis, we examined group data of impedance normalized to its value in the first session. We compared groups of electrodes that underwent stimulation with those that did not. For this analysis, electrodes with impedance values below 5 kΩ or above 500 kΩ in the first session were excluded from both groups. This method of analysis is akin to that performed by Chen et al., particularly depicted in Figure 3A of their paper [10]. In that figure, the impedances of implanted UEAs electrodes decrease over time to reach 50% to 70% of the initial impedance after approximately 15 weeks. This trend is observed for both unstimulated electrodes and electrodes chronically stimulated at relatively low charge levels. However, data from the cat implanted with SiC insulation suggests that impedances increase over time. Stimulated electrodes exhibit less growth in impedance compared to unstimulated electrodes (Figure 10). Around the 13-week mark, impedances of stimulated electrodes increased by approximately 20% more than their initial values. Unstimulated electrodes also showed increases in impedance, but the progression of changes is not as systematic.

CONCLUSIONS

Our preliminary results with a-SiC coated UEAs are very promising. This study demonstrates that SiC yields more stable performance and maintains stable impedance over time both in in vitro and in vivo settings. This superior performance suggests the potential usefulness of SiC for chronic implants.

DISCLAIMER

Florian Solzbacher has a financial interest in Blackrock Neurotech, a company that develops and manufactures implantable neural interfaces utilized in this study.

ACKNOWLEDGEMENTS

Research reported in this publication was supported by the National Institute on Deafness and Other Communication Disorders of the National Institutes of Health under Award Number R44DC018261. The content is solely the responsibility of the authors and does not necessarily represent the official views of the National Institutes of Health.

REFERENCES

[1] J. C. Barrese, N. Rao, K. Paroo, C. Triebwasser, C. Vargas-Irwin, L. Franquemont, and J. Donoghue, "Failure mode analysis of silicon-based intracortical microelectrode arrays in non-human primates," *Journal of Neural Engineering*, vol.10, 066014, (2013).

[2] J.-M. Hsu, L. Rieth, R. A. Normann, P. Tathireddy, and F. Solzbacher, "Encapsulation of an integrated neural interface device with parylene-C," *IEEE Trans. Biomed. Eng*. 55, 1–7 (2008).

[3] R. Bhandari, S. Negi, and F. Solzbacher, "Wafer-scale fabrication of penetrating neural microelectrode arrays," *Biomed. Microdevices,* vol. 12, no. 5, pp. 797–807, (2010).

[4] S. Negi, R. Bhandari, L. Rieth, and F. Solzbacher, "In vitro comparison of sputtered iridium oxide and platinum-coated neural implantable microelectrode arrays," *Biomedical Materials*, 5(1), 015007, (2010).

[5] S. Negi, R. Bhandari, L. Rieth, R. V, Wagenen, and F. Solzbacher, "Neural electrode degradation from continuous electrical stimulation: comparison of sputtered and activated iridium oxide, *Journal of Neuroscience Methods*, 186(1), pp. 8-17, (2010).

[6] X. Lei, S. Kane, S. Cogan, H. Lorach, L. Galambos, P. Huie, K. Mathieson, T. Kamins, J. Harris, and D. Palanker, "SiC protective coating for photovoltaic retinal prosthesis," *Journal of Neural Engineering*, vol. 13, no. 4, (2016).

[7] A. Joshi-Imre, B. J. Black, J. Abbott, A. Kanneganti, R. Rihani, B. Chakraborty, V. R. Danda, J. Maeng, R. Sharma, L. Rieth, "Chronic recording and electrochemical performance of amorphous silicon carbide-coated Utah electrode arrays implanted in rat motor cortex," *Journal of Neural Engineering,* vol. 16, no. 4, p. 046006, (2019).

[8] C. K. Nguyen, J. R. Abbott, S. Negi, and S. F. Cogan, "Evaluation of Amorphous Silicon Carbide on Utah Electrode Arrays by Thermal Accelerated Aging," 43rd Annual International Conference of the IEEE Engineering in Medicine and Biology Society (EMBC), (2021), pp. 6623-6626.

[9] J. Meng, B. Chakraborty, N. Geramifard, T. Kang, R. T. Rihani, A. Joshi-Imre, S. F. Cogan, "High-charge-capacity sputtered iridium oxide neural stimulation electrodes deposited using water vapor as a reactive plasma constituent," *J. Biomed. Mater. Res. Part B Appl. Biomater.*, vol. 108, no. 3, pp. 880–891, (2019).

[10] K. H. Chen, J. F. Dammann, J. L. Boback, F. V. Tenore, K. J. Otto, R. A. Gaunt, and S. Bensmaia, "The effect of chronic intracortical microstimulation on the electrode-tissue interface," *Journal of Neural Engineering*, vol 11, pp, 026004, (2014).

CONTACT

*Sandeep Negi, tel: +1-801-231-7085; snegi@blackrockneuro.com